

Supporting Information: Disparity in anomalous diffusion of proteins searching for their target DNA sites in a crowded medium is controlled by size, shape and mobility of macromolecular crowders

Pinki Dey and Arnab Bhattacharjee*

School of Computational and Integrative Sciences, Jawaharlal Nehru University, New Delhi-
110067, India

List of contents:	Page no.
1. Simulation models	1-5
a. Protein model.	1-3
b. DNA model.	3-5
c. Crowder model.	5
d. Polymeric crowder model.	5
e. Protein-DNA interactions.	6
2. System Configuration and Preparation	7
3. Criteria for data analysis	7
4. Tables	8-9
5. Figures	9-15
6. References	15-16

1. Simulation models.

a. Protein model: The protein used for our study is Sap-1(PDB ID: 1BC8). It is a member of Ets transcription factor and binds to a 9-bp DNA target site located in *c-fos* promoters¹. The protein is a 93-amino acid long single domain transcription factor and contains a

well-defined recognition helix which is used to scan and bind specifically to the target DNA site. The folded structure of the protein throughout the simulation is ensured by a structure based Leonard-Jones potential². Moreover, the electrostatic interactions between the negatively charged amino acids (Glu and Asp) and the positively charged amino acids (Arg and Lys) are modelled by Debye-Huckel potential. Although, the application of Debye-Huckel potential is limited to dilute ion solutions, it is quite successful to predict many crucial aspects of nuclear acid biophysics^{3,4}.

The potential to model the protein molecule is given as,

$$E_{pot} = E_{bond} + E_{bend} + E_{torsion} + E_{LJ} + E_{ev} + E_{ele} \quad (1)$$

E_{bond} gives the bonded energy as,

$$E_{bond} = \sum_i k_b (r_i - r_i^0)^2 \quad (2)$$

where $k_b = 100.0$ kcal/mol/Å², r_i and r_i^0 represents the distances between i -th and $i+1$ -th C_α beads in an intermediate and the folded structures of the protein respectively.

E_{bend} represents the potential energy function for any variation in angles and is given as,

$$E_{bend} = \sum_i k_\theta (\theta_i - \theta_i^0)^2 \quad (3)$$

where $k_\theta = 20.0$ kcal/mol/rad², θ_i and θ_i^0 represents the angles among i -th, $i+1$ -th, $i+2$ -th C_α beads in an intermediate and the folded structures of the protein respectively.

$E_{torsion}$ gives the potential energy function for torsional angle between four atoms connected by bonds and is given as,

$$E_{torsion} = \sum_i \{k_{\phi_1} [1 - \cos 3(\phi_i - \phi_i^0)] + k_{\phi_2} [1 - \cos(\phi_i - \phi_i^0)]\} \quad (4)$$

where $k_{\phi_1} = 0.5$ kcal/mol, $k_{\phi_2} = 1.0$ kJ/mol, ϕ_i and ϕ_i^0 are the torsional angles between i -th, $i+1$ -th, $i+2$ -th, $i+3$ -th C_α beads in an intermediate and the folded structures of the protein respectively.

E_{LJ} estimates the conformational energy using a native topology based model² in which a Lennard-Jones potential favours the formation of contacts found in the folded structure of the protein.

$$E_{LJ} = \sum_{i < j-3}^{native} \epsilon_{ij} \left[5 \left(\frac{\sigma_{ij}}{r_{ij}} \right)^{12} - 6 \left(\frac{\sigma_{ij}}{r_{ij}} \right)^{10} \right] \quad (5)$$

where $\epsilon_{ij} = 3.824091778$ kcal/mol. r_{ij} and σ_{ij} represent the distances between the native pairs in a snapshot generated at a given time and in the folded structure respectively.

E_{ev} represents the excluded volume interactions between all non-bonded and non-native pairs of protein and also between the protein and DNA and is given as,

$$E_{ev} = \sum_{i < j-3}^{non-native} \epsilon_{ev} \left(\frac{\sigma_{ij}}{r_{ij}} \right)^{12} \quad (6)$$

where $\epsilon_{ev}=0.239$ kcal/mol, r_{ij} represents the distance between i -th and j -th beads and $\sigma_{ij} = \sigma_i + \sigma_j$ gives the interaction specific length scale, where σ_i and σ_j are the radii of the interacting beads.

E_{elec} models the electrostatic interactions and is given by Debye-Hückel potential as,

$$E_{elec} = \sum_{i < j} \frac{q_i q_j e^{-r_{ij}/\lambda_D}}{4\pi\epsilon_0\epsilon(T,C)r_{ij}} \quad (7)$$

where q_i and q_j are the charges on site i and j , r_{ij} is the separation between the two sites. $\epsilon(T, C)$ represents the dielectric permittivity of solution and is a function of the molarity of NaCl and temperature⁴ as

$$\epsilon(T, C) = \epsilon(T) a(C),$$

$$\epsilon(T) = 249.4 - 0.788 T/K + 7.20 \times 10^{-4} (T/K)^2 \text{ and,}$$

$$a(C) = 1.00 - 2.551 C/M + 5.151 \times 10^{-2} (C/M)^2 - 6.889 \times 10^{-3} (C/M)^3$$

The Debye screening length is given as;

$$\lambda_D = \sqrt{\frac{\epsilon_0 \epsilon(T, C)}{2 \beta N_A e^2 I}}$$

β represents the inverse thermal energy of the system $(k_B T)^{-1}$, k_B is Boltzmann constant, N_A is Avogadro's number, and I is the ionic strength of solution.

b. DNA model: The 3SPN.2 model by Pablo et.al⁵ has been used to describe the DNA force field. Here, each nucleotide is represented by three beads placed at the centre of masses of phosphate, sugar and base respectively. This model provides correct description of structural properties such as, major and minor grooves and is consistent with experimental measures. The ability of this model to capture a correct persistence length for both ss- and ds-DNA and to predict melting temperatures in agreement with experimental results make it a suitable candidate to study the molecular basis of DNA dynamics.

According to the model, the total potential energy function of the DNA is given as,

$$E_{pot}^{DNA} = E_{bond}^{DNA} + E_{bend}^{DNA} + E_{tors}^{DNA} + E_{exe}^{DNA} + E_{bstk}^{DNA} + E_{cstk}^{DNA} + E_{bp}^{DNA} + E_{elec}^{DNA} \quad (8)$$

E_{bond}^{DNA} gives the bonding energy as,

$$E_{bond}^{DNA} = \sum_i k_b (r_i - r_i^0)^2 + 100k_b (r_i - r_i^0)^4 \quad (9)$$

where $k_b = 0.6 \text{ kJ/mol/\AA}^2$ and r_i, r_i^0 represent the instantaneous and equilibrium bond length for i -th bond respectively.

E_{bend}^{DNA} represents the energy function for bending and is given as,

$$E_{DNA}^{bend} = \sum_i k_\theta (\theta_i - \theta_i^0)^2 \quad (10)$$

Where $k_\theta = 200 \text{ kJ/mol/rad}^2$, θ_i^0 are the instantaneous and equilibrium bond angles for the i -th bond angle respectively.

E_{tors}^{DNA} represents the potential energy function for torsional angle between every four atoms connected by bonds,

$$E_{tors}^{DNA} = \sum_i -k_\phi \exp\left(\frac{-(\phi_i - \phi_i^0)^2}{2\sigma_{\phi,i}^2}\right) \quad (11)$$

where $k_\phi = 6.0 \text{ kJ/mol}$, ϕ_i, ϕ_i^0 and $\sigma_{\phi,i}$ represents the well-depth, equilibrium angle, and Gaussian well-width of dihedral i respectively.

E_{exe}^{DNA} is the energy function for excluded volume of purely repulsive potential between sites i and j ,

$$E_{exe}^{DNA} = \sum_{i < j} \begin{cases} \epsilon_r \left[\left(\frac{\sigma_{ij}}{r_{ij}} \right)^{12} - 2 \left(\frac{\sigma_{ij}}{r_{ij}} \right)^6 \right] + \epsilon_r, & r < r_c \\ 0 & r \geq r_c \end{cases} \quad (12)$$

where $\epsilon_r = 1.0 \text{ kJ/mol}$ is the energy parameter, σ_{ij} is the average site diameter between i and j , and r_{ij} is the separation between them. r_c represents the cutoff distance for the excluded volume interactions.

E_{bstk}^{DNA} gives the potential energy for intra-stand Base-stacking as,

$$E_{bstk}^{DNA} = \sum_{bstk} \begin{cases} U_m^{rep}(\epsilon_{ij}, \alpha_{BS}, r_{ij}) + (K_{BS}, \Delta\theta_{BSij}) U_m^{attr}(\epsilon_{ij}, \alpha_{BS}, r_{ij}) & r_{ij} < r_{ij}^0 \\ f(K_{BS}, \Delta\theta_{BSij}) U_m^{attr}(\epsilon_{ij}, \alpha_{BS}, r_{ij}) & r_{ij} \geq r_{ij}^0 \end{cases} \quad (13)$$

where $K_{BS} = 6.0$, $\alpha_{BS} = 3.0$ and ϵ_{ij} denotes the depth of the well of attraction between sites i and j , r_{ij}^0 is the equilibrium separation between the sites, and α_{BS} is used to adjust the range of attraction. f is used to modulate the decomposition of attractive and repulsive portions of Morse potential. The interactions of base stacking are modulated by f using θ_{BS}

E_{bp}^{DNA} gives the potential energy function for base pairing (14)

$$E_{bp}^{DNA} = \sum_{bp} \begin{cases} U_m^{rep}(\epsilon_{ij}, \alpha_{BP}, r_{ij}) + \frac{1}{2}(1 + \cos(\Delta\phi_i))f(K_{BP}, \Delta\theta_{1ij})f(K_{BP}, \Delta\theta_{2ij})U_m^{attr}(\epsilon_{ij}, \alpha_{BP}, r_{ij}) & r_{ij} < r_{ij}^0 \\ \frac{1}{2}(1 + \cos(\Delta\phi_i))f(K_{BP}, \Delta\theta_{1ij})f(K_{BP}, \Delta\theta_{2ij})U_m^{attr}(\epsilon_{ij}, \alpha_{BP}, r_{ij}) & r_{ij} \geq r_{ij}^0 \end{cases}$$

where $K_{BP}=12.0$, $\alpha_{BP}=2.0$ and ϵ_{ij} denotes the depth of the well of attraction between i and j , r_{ij}^0 is the equilibrium separation between the sites, and the parameter, α_{BP} is used to control the range of attraction. f modulates the decomposition of attractive and repulsive portions of the Morse potential, $\Delta\phi_1 = \phi_1 - \phi_1^0$ is used to penalize deviations from a reference dihedral angle. Due to this decomposition, the repulsive character is maintained. f using θ_1 and θ_2 modulates the base pairing interactions.

E_{cstk}^{DNA} gives the potential energy function for cross stacking,

$$E_{cstk}^{DNA} = \sum_{cstk} f(K_{BP}, \Delta\theta_{3ij})f(K_{CS}, \Delta\theta_{CSij})U_m^{attr}(\epsilon_{ij}, \alpha_{CS}, r_{ij}) \quad (15)$$

where $K_{CS}= 8.0$, $\alpha_{CS}= 4.0$ and ϵ_{ij} denotes the depth of well of attraction between sites i and j . The modulation in cross stacking interaction is achieved using both θ_3 and θ_{CS} .

E_{elec}^{DNA} denotes a screened electrostatic potential between intra-strand and inter-strand phosphates and is modelled by using the potential energy function in Eqn. (7).

c. Crowder model: Crowders are modelled as uncharged spheres occupying a volume fraction, $\phi = 4N_c\pi R^3/3 L_x L_y L_z$. Here, L_x , L_y and L_z are the dimensions of simulation box used with a periodic boundary condition, N_c denotes total number of crowders and R is the radius of each crowder. The crowders are randomly placed inside the simulation box and interact only through nonspecific excluded volume interaction which is modelled by Lennard-Jones potential⁶,

$$E_{LJ} = \sum_{i < j} \begin{cases} k_{ev} \left[\left(\frac{\sigma_{ij}}{r_{ij}} \right)^{12} - 2 \left(\frac{\sigma_{ij}}{r_{ij}} \right)^6 + 1 \right], & r < r_c \\ 0 & r \geq r_c \end{cases}$$

where $k_{ev}=0.239005736$ kcal/mol denotes the energy parameter, σ_{ij} is the average site diameter, and r_{ij} is the separation between sites i and j . r_c denotes the cut off distance.

d. Polymeric crowder model: We constructed random polymeric chains by threading beads together through a simple harmonic potential given as,

$$E_{bond} = \sum_i k_b (r_i - r_i^0)^2$$

where $k_b = 23.900573614$ kcal/mol/Å², r_i and r_i^0 represents the distances between i -th and $i+1$ -th crowder respectively. The length of the crowder chain is varied by varying the number of constituting beads, where radius of each bead is taken as 10 Å and mass as 110 Da. We constructed polymeric crowders of length 5, 10, 15, 20, 25 and 30.

e. Protein-DNA interaction: In our model, protein and DNA are allowed to interact through two modes of interactions:

(i) Non-specific interactions: The Sap-1 protein non-specifically scans the DNA in quest of the target DNA site. During this process, two main interactions come into play. One is the electrostatic interaction between the charged amino acids and the phosphates present in DNA. Another nonspecific interaction is the excluded volume interaction between them. The electrostatic interaction is modelled using Debye-Huckel potential (Eqn.7) and excluded volume interactions are modelled using Eqn.6.

(ii) Specific protein-DNA interactions: When the protein reaches the target site, it binds specifically to the major groove using its recognition helix. The required information regarding the specific contacts are obtained from the X-ray crystallographic structure of Sap-1 (PDB ID: 1BC8). The formation of specific contacts are modelled using a short-ranged Lennard-Jones potential as,

$$E_{LJ} = \sum_{i < j} \begin{cases} k_{sp} \left[5 \left(\frac{\sigma_{ij}}{r_{ij}} \right)^{12} - 6 \left(\frac{\sigma_{ij}}{r_{ij}} \right)^{10} \right], & r < r_c \\ 0, & r \geq r_c \end{cases}$$

where $k_{sp}=0.5$ kcal/mol, σ_{ij} denotes the average site diameter between sites i and j , while r_{ij} is the separation between them. r_c denotes the cut off distance at $(\sigma_{ij}+5)$ Å.

2. System configuration and Preparation:

The coarse-grained model of the protein is generated from the atomic coordinates of the crystal structure, 1bc8.pdb. The 100 bp B-DNA structure, obtained from w3DNA (3D DNA structure) web server (<http://w3dna.rutgers.edu>), provides the template for generation of coarse-grained model of DNA. The DNA is placed in the middle of the simulation box with a box size of 150Å X 150Å X 410Å. The formation of specific contacts are ensured by inserting a 9 bp target DNA sequence as found in the crystal structure of sap-1 in the present DNA model. Initially, the protein is placed far from the DNA surface and the crowders are distributed randomly inside the simulation box.

The dynamics of the protein in the crowded environment was simulated using Langevin dynamics simulation with friction coefficient, $\gamma=0.05$ at a temperature of 300K under physiological salt concentration of 140mM. 20 independent simulations of 1×10^8 MD steps long (100μs) are carried out for each crowded system in order to achieve significant statistics.

The sizes and masses of macromolecular crowding agents used in our study correspond to PEG crowders⁷ used in experimental studies. In order to incorporate the size effect, we kept the mass constant at 1000Da and varied the radii from the 7.8Å to 21Å. The mass effect is studied by changing the mass of the crowders from 10KDa to 40KDa at a radius of 21Å. Moreover, crowder polymers of 5,10,15,20 crowder repeats are modelled to study the effect of polymer crowding. Each crowder in the polymer chains have a radius of 10Å and mass 110 Da.

3. Criteria for data analysis:

The protein is said to perform 1D diffusion if it either slides or hops along the DNA surface. Sliding is confirmed in a snapshot if at least 70% of the recognition helix is within the DNA major groove and the centre of mass of the recognition helix is within 18Å to the nearest DNA base pair with an orientation angle $< 25^\circ$. Hopping is considered if the recognition helix is within 30Å from the DNA but don't match any of the criteria for sliding. The protein performs 3D diffusion when the recognition region of the protein is at least 25Å away from the nearest DNA base pair.

Calculation of depletion region around DNA:

The depletion region around the DNA molecule is calculated by measuring the distance between the centre of each DNA base pair and the crowder molecule nearest to it throughout the simulation.

Calculation of effective diffusion coefficient:

In Fig.2 the mean square displacement (MSD) data at varying radius, mass and crowder polymer length for 3D diffusion are presented for long time scale. Here, the method^{8,9} adopted for calculation of 1D diffusion coefficient is by plotting the logarithmic of (MSD/2t) against the logarithmic of time. Similarly, for the calculation of 3D diffusion coefficient, the logarithmic of (MSD/6t) is plotted against the logarithmic of time over a long-time scale since $\ln(\text{MSD}/6t)$ reaches a plateau value. The exact value of $\ln(\text{MSD}/6t)$ at this plateau gives the measure of $\ln(D^{\text{eff}})$. This method helps us to visualize if the simulation has reached a sufficient long time scale¹⁰.

Calculation of ruggedness chemical potential landscape:

To calculate the roughness of the chemical energy landscape, we followed the method adopted by Szleifer et al¹⁰. Here, we divided our simulation box into small cubic cells of side 50Å where the diffusing particle (Sap-1 protein) can move from each cell to another. While diffusing through the cells, the protein feels an effective potential, which is protein's excess chemical potential. Therefore, by calculating the standard deviation of the average of each cell's potential gives a measure of ruggedness of the potential energy landscape.

The ruggedness of the chemical potential landscape is calculated as,

$$\sigma[\ln(p^{\text{cell}})] = \sqrt{\frac{1}{N_{\text{cells}}} \sum_i \left(\ln(p_i^{\text{cell}}) - \overline{\ln(p_i^{\text{cell}})} \right)^2}$$

Where, p_i^{cell} is the probability of the protein to be present in cell i . N_{cells} is the number of cubic cells present inside the simulation box.

4. Tables

Table1: Masses and Radius used for DNA components:

	Mass (Da)	Radius(Å)
Phosphate	94.97	2.25
Sugar	83.11	3.20
Adenine(A)	134.1	2.70
Thymine(T)	125.1	3.55
Guanine(G)	150.1	2.45
Cytosine(C)	110.1	3.20

Table 2: Masses and Radius used for amino acids:

Amino acid (single-letter code)	Mass (Da)	Radius of C _α (Å)
Isoleucine (I)	131.1	2.0
Lysine(K)	146.1	2.0
Phenylalanine(F)	165.2	2.0
Threonine(T)	119.1	2.0
Tryptophan(W)	204.2	2.0
Valine(V)	117.1	2.0
Arginine(R)	174.2	2.0
Histidine (H)	155.1	2.0
Alanine(A)	89.0	2.0
Asparagine(N)	132.1	2.0
Leucine (L)	131.1	2.0
Methionine(M)	149.2	2.0
Aspartic Acid (D)	133.1	2.0
Cytosine (C)	121.1	2.0
Glutamic acid (E)	147.1	2.0
Glutamine (Q)	146.1	2.0
Glycine (G)	75.0	2.0
Proline (P)	115.1	2.0
Serine (S)	105.0	2.0
Tyrosine(Y)	181.1	2.0

Table 3: List of various sizes of PEG crowders as obtained from Sabirov et al⁷.

PEG crowders	Hydrodynamic radius(nm)
PEG600	0.78
PEG1000	0.94
PEG1450	1.05
PEG2000	1.22
PEG3000	1.44
PEG3400	1.63
PEG4600	2.1
PEG6000	2.5
PEG20000	5.1

Table 4: Crowder Radius used in simulation at Mass 68kDa:

In order to incorporate the size effect of macromolecular crowding on the target search dynamics of DBPs, we keep the crowder mass constant at 68kDa and vary the radii from the 7.8Å to 21Å.

Radius(Å)	7.8	10	12.2	14.4	16.3	21
-----------	-----	----	------	------	------	----

Table 5: Crowder masses used in simulations at Radii 21.0Å:

In order to incorporate the effect of mobility of macromolecular crowding on the target search dynamics of the searching protein, we fix the crowder radius at 21Å and change the mass from the 2 kDa to 68 kDa.

Mass(kDa)	2	10	15	20	25	30	40	50	68
-----------	---	----	----	----	----	----	----	----	----

5. Figures:

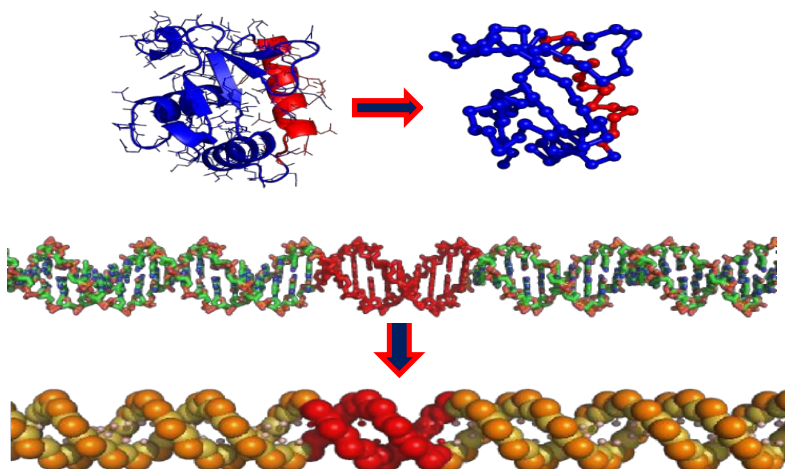


Figure S1: Schematic representation of Sap-1 and B-DNA molecule in all atom (top left and middle) and coarse-grained (top right and bottom) models. The Sap-1 recognition helix is highlighted with red colour and corresponds to 53-68 amino acids in the protein. Each nucleotide in the coarse grained model of DNA is presented by three beads at the centre of phosphate (orange colour beads), sugar (yellow colour beads) and base (pink colour beads). The 9 base pair DNA target site region is represented with red colour.

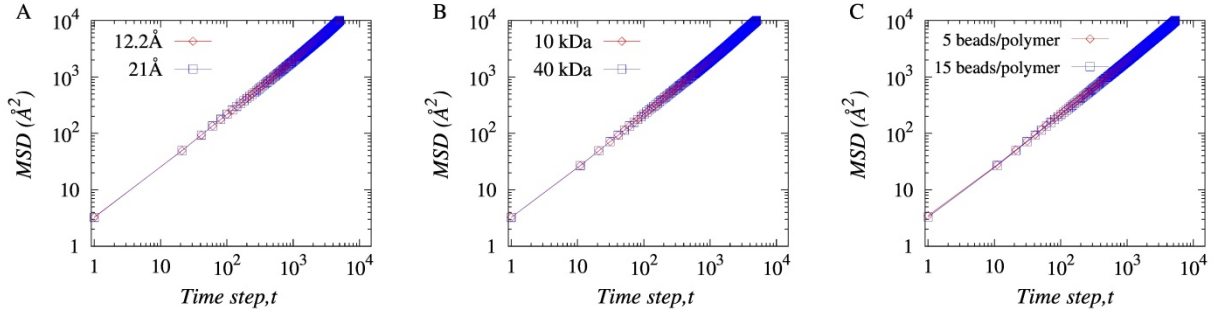


Figure S2. Variation in the long-time average raw MSD data during 1D diffusion of the protein diffusing inside the depletion region for (A) three two crowder radii, 12.2Å and 21Å at a fixed mass of 68kDa. (B) two different crowder masses, 10kDa and 40kDa at a fixed radius of 21 Å and (C) two types of polymeric crowders, 5 and 15 beads per polymer.

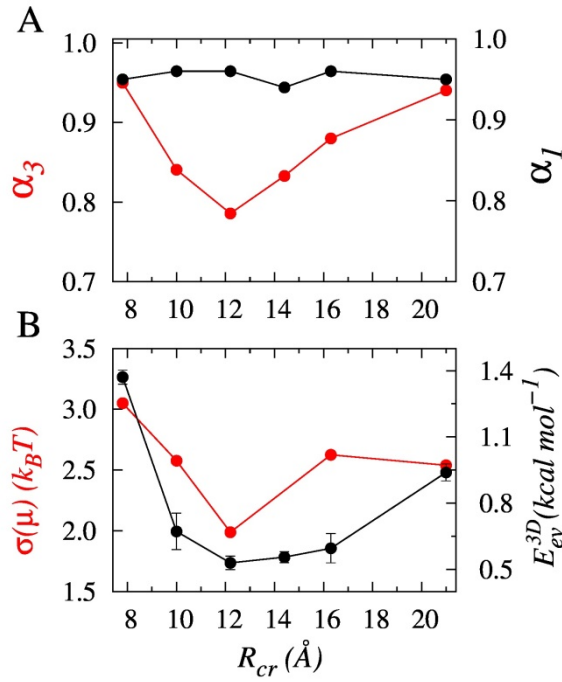


Figure S3: Impact of varying crowder size on the diffusion of DBP keeping the crowder mass fixed at 1kDa. (A) Variation in the 1D and 3D diffusion exponent, α_1 (black line) and α_3 (red line) respectively concerning the change in crowder size from 7.8Å to 21Å. (B) Estimation of protein-crowder excluded volume interaction (black line) and ruggedness of potential energy landscape (red line) as a function of increasing crowder size.

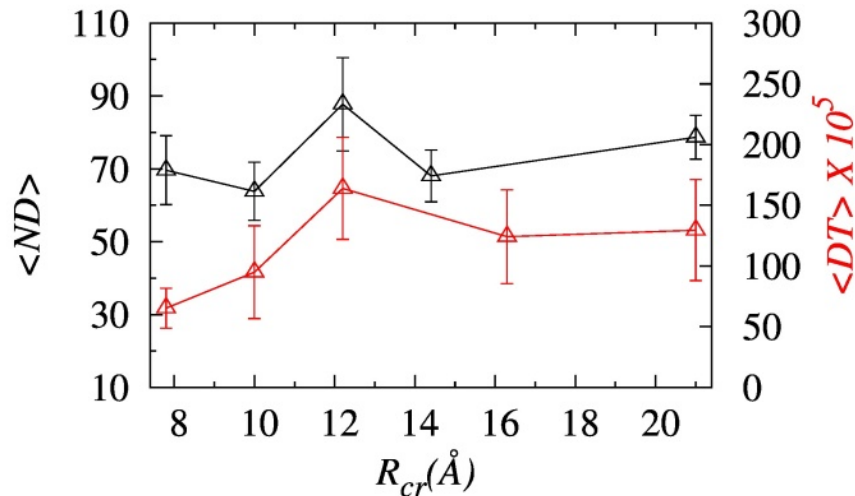


Figure S4: The figure represents the variation in the average number of diffusion events ($\langle ND \rangle$) and the average time spent during each diffusion event ($\langle DT \rangle$) as a function of crowder size. Here, we see that the average number of diffusion events as well as the diffusion time increases at a crowder size of 12.2Å leading to enhanced 3D diffusion.

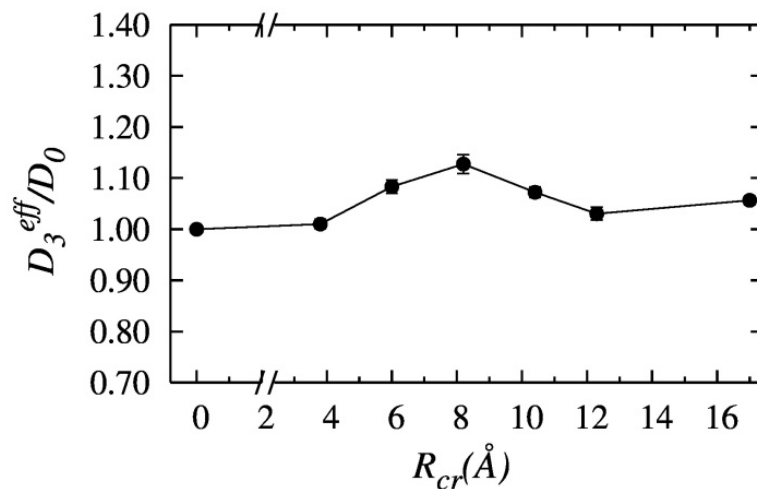


Figure S5: The representative figure shows the variation in the effective 3D-diffusion coefficient normalized by its value in the absence of crowders as a function of macromolecular crowding size keeping the crowder mass constant at 68kDa.

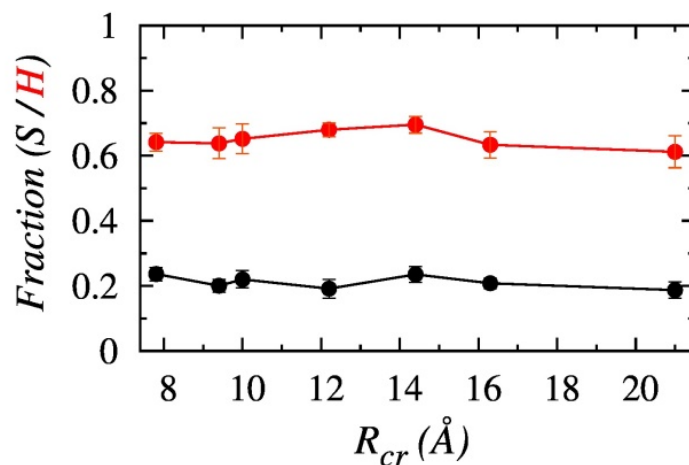


Figure S6: The above figure presents the effect of increasing crowder size on non-specific sliding (S) and hopping (H) dynamics of the DBP at 140 mM salt concentration. During the non-specific search, the variation in the sliding and hopping search modes is very insignificant as a function of crowder size.

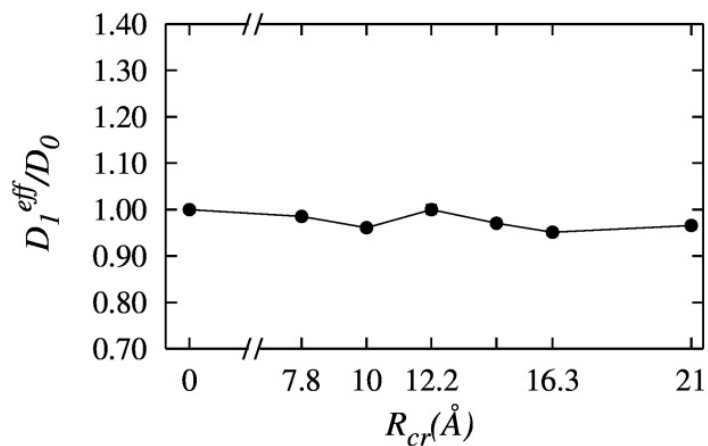


Figure S7: The above figure shows the variation in the effective 1D-diffusion coefficient normalized by its value in the absence of crowders as a function of size of macromolecular crowding agents keeping the crowder mass constant at 68kDa.

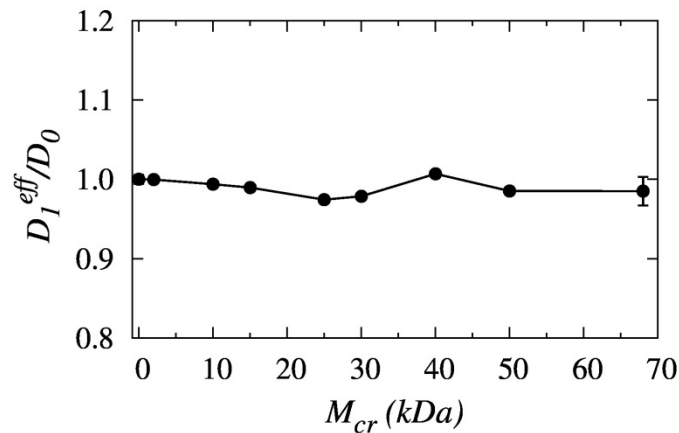


Figure S8: The above figure shows the variation in the effective 1D-diffusion coefficient normalized by the 1D-diffusion coefficient in the absence of crowders as a function of mass of macromolecular crowding agents keeping the radius constant at 21Å.

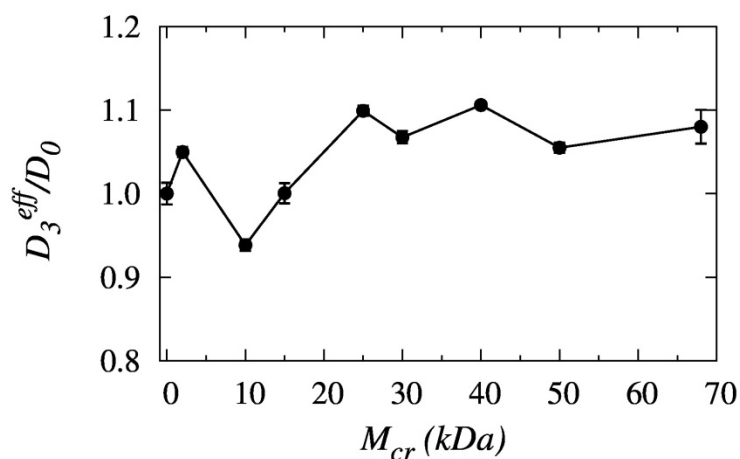


Figure S9: The representative figure shows the variation in the effective 3D-diffusion coefficient normalized by its value in the absence of crowders as a function of mass of macromolecular crowding agents keeping the crowder radius constant at 21Å. Here, the effective 3D diffusion coefficient drops to a minimum value when the crowder mass is ~10kDa which matches with the mass of Sap-1 protein used.

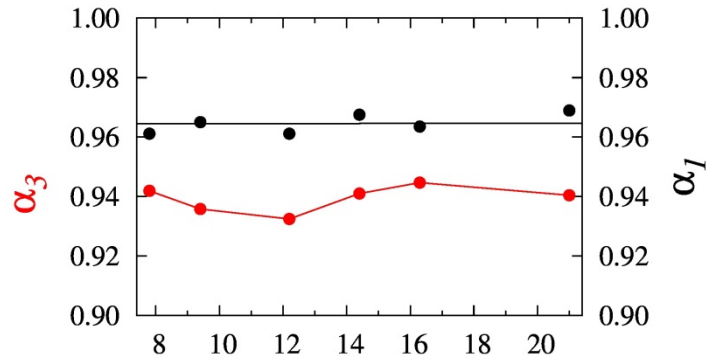


Figure S10: The representative figure shows the variation in the 1D and 3D diffusion exponent, α_1 (black line) and α_3 (red line) respectively as a function of crowder size and mass consistent with the PEG crowders⁷.

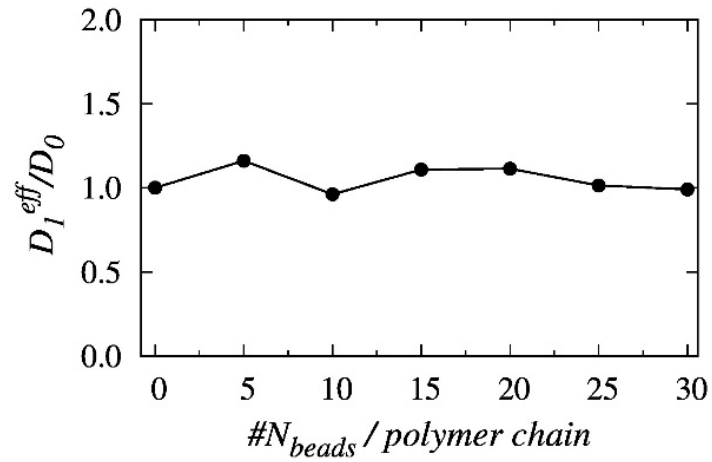


Figure S11: The representative figure shows the variation in the effective 1D-diffusion coefficient normalized by the 1D-diffusion coefficient in the absence of crowders as a function of polymeric crowder length. Each bead in the polymer has a mass of 110Da and radius of 10Å.

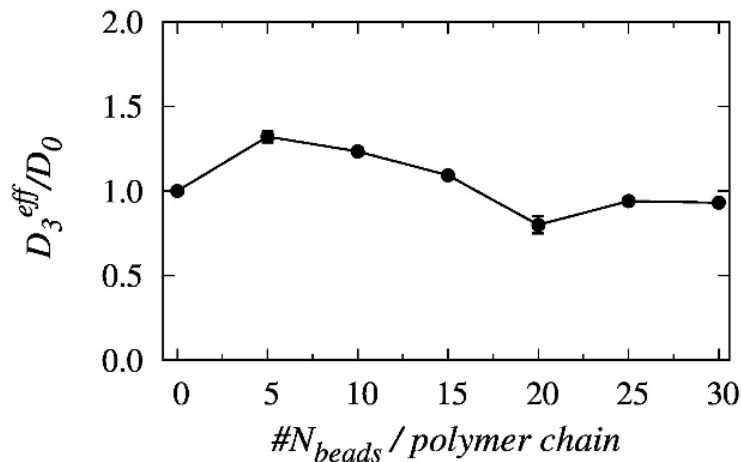


Figure S12: The above figure shows the variation in the effective 3D-diffusion coefficient normalized by its value in the absence of crowders as a function of polymeric crowder length.

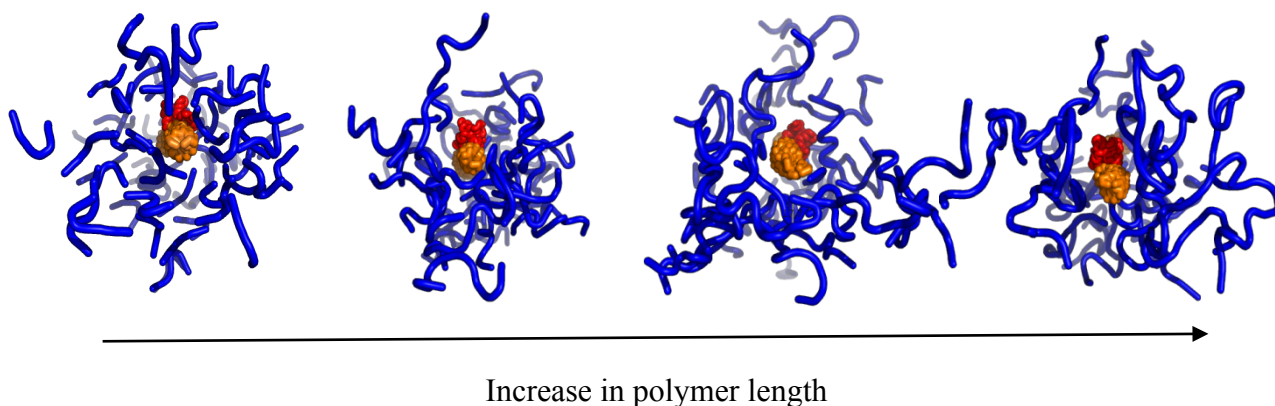


Figure S13: Schematic representation showing the increase in entanglement of crowder polymers as we increase the polymer length. This increasing entanglement of polymer crowders traps the searching protein when it performs 3D diffusion in the bulk solution leading to enhanced cross talks/excluded volume interactions between them.

References:

- (1) Mo, Y.; Vaessen, B.; Johnston, K.; Marmorstein, R. Structures of SAP-1 Bound to DNA Targets from the E74 and c-Fos Promoters: Insights into DNA Sequence Discrimination by Ets Proteins. *Mol. Cell* **1998**, 2 (2), 201–212.

- (2) Clementi, C.; Nymeyer, H.; Onuchic, J. N. Topological and Energetic Factors: What Determines the Structural Details of the Transition State Ensemble and “En-Route” Intermediates for Protein Folding? An Investigation for Small Globular Proteins. *J. Mol. Biol.* **2000**, *298* (5), 937–953.
- (3) Mondal, A.; Bhattacharjee, A. Searching Target Sites on DNA by Proteins : Role of DNA Dynamics under Confinement. **2015**, 1–11.
- (4) Azia, A.; Levy, Y. Nonnative Electrostatic Interactions Can Modulate Protein Folding: Molecular Dynamics with a Grain of Salt. *J. Mol. Biol.* **2009**, *393* (2), 527–542.
- (5) Hinckley, D. M.; Freeman, G. S.; Whitmer, J. K.; Pablo, J. J. De; Hinckley, D. M.; Freeman, G. S.; Whitmer, J. K.; De, J. J. An Experimentally-Informed Coarse-Grained 3-Site-per-Nucleotide Model of DNA: Structure, Thermodynamics, and Dynamics of Hybridization. *J. Chem. Phys.* **2013**, *139*, 144903.
- (6) Ma, Y.; Chen, Y.; Yu, W.; Luo, K.; Ma, Y.; Chen, Y.; Yu, W.; Luo, K. How Nonspecifically DNA-Binding Proteins Search for the Target in Crowded Environments How Nonspecifically DNA-Binding Proteins Search for the Target in Crowded Environments. *J. Chem. Phys.* **2016**, *144* (12), 125102.
- (7) Sabirov, R. Z.; Krasilnikov, O. V.; Ternovsky, V. I.; Merzliak, P. G. Relation between Ionic Channel Conductance and Conductivity of Media Containing Different Nonelectrolytes. A Novel Method of Pore Size Determination. *Gen. Physiol. Biophys.* **1993**, *12* (2), 95–111.
- (8) Saxton, M. J. Anomalous Diffusion Due to Obstacles: A Monte Carlo Study. *Biophys. J.* **1994**, *66* (2), 394–401.
- (9) Vilaseca, E.; Isvoran, A.; Madurga, S.; Pastor, I.; Garcés, J. L.; Mas, F. New Insights into Diffusion in 3D Crowded Media by Monte Carlo Simulations: Effect of Size, Mobility and Spatial Distribution of Obstacles. *Phys. Chem. Chem. Phys.* **2011**, *13* (16), 7396–7407.
- (10) Garb, G.; Tagliazucchi, M.; Szleifer, I. Supplementary Materials : Nonmonotonic Diffusion in Crowded Environments. **2014**.